Role of MgATP and MgADP in the cross-bridge kinetics in chemically skinned rabbit psoas fibers

Study of a fast exponential process (C)

Masataka Kawai* and Herbert R. Halvorson‡

*Department of Anatomy, The University of Iowa, Iowa City, Iowa 52242; and ‡Division of Physical Biochemistry, Henry Ford Hospital, Detroit, Michigan 48202

ABSTRACT The role of the substrate (MgATP) and product (MgADP) molecules in cross-bridge kinetics is investigated by small amplitude length oscillations (peak to peak: 3 nm/cross-bridge) and by following amplitude change and phase shift in tension time courses. The range of discrete frequencies used for this investigation is 0.25–250 Hz, which corresponds to 0.6–600 ms in time domain. This report investigates the identity of the high frequency exponential advance (process C), which is equivalent to "phase 2" of step analysis. The experiments are performed in maximally activated (pCa 4.5–5.0) single fibers from chemically skinned rabbit psoas fibers at 20°C and at the ionic strength 195 mM. The rate constant $2\pi c$ deduced from process (C) increases and saturates hyperbolically with an increase in MgATP concentration, whereas the same rate constant decreases monotonically with an increase in MgADP concentration. The effects of MgATP and MgADP are opposite in all respects we have studied. These observations are consistent with a cross-bridge scheme in which MgATP and MgADP are in rapid equilibria with rigorlike cross-bridges, and they compete for the substrate site on myosin heads. From our measurements, the association constants are found to be 1.4 mM^{-1} for MgATP and 2.8 mM^{-1} for MgADP. We further deduced that the composite second order rate constant of MgATP binding to cross-bridges and subsequent isomerization/dissociation reaction to be $0.57 \times 10^6\ M^{-1}s^{-1}$.

INTRODUCTION

Characterizing the steps of a mechanism that describes force generation in muscle is of appreciable interest. We approach this problem by following tension transients which are induced by length changes on active muscles. If the change is a step increase in length, the tension changes simultaneously with the length change (phase 1), and this is followed by relaxation time courses involving two or three exponentials (phases 2–4; Huxley and Simmons, 1971; Heinl et al., 1974). Based on the asymmetry of the rate constant of phase 2, Huxley and Simmons constructed a cross-bridge model which mapped phase 2 to the step involved in force generation. This step is generally referred to as the power stroke. It is now known that no large rotation in the myosin head takes place with the power stroke as was originally conceived (Yanagida, 1981; Cooke et al., 1982; reviewed by Thomas, 1987). The central assumption in the Huxley-Simmons model is that the length alteration modifies the rate constant of the reaction which produces the power stroke, and an early appproach to the steady state yields a transient identified as phase 2.

We have been studying transients by sinusoidal length alterations, and by following the concurrent time courses in tension. The sinusoidal waveform provides the advantage of greater temporal resolving power. It is also advantageous that some high-frequency artifacts, such as the longitudinal propagation of contraction waves (Sugi and Kobayashi, 1983) and oscillatory pickup by force transducer on sudden length change, can be minimized. With sinusoidal analysis, we identified an exponential lead (of tension over length) at frequencies centering around 70 Hz, and named it process (C). It is possible to show both mathematically and empirically that process (C) is equivalent to phase 2 of the step analysis. We found that the rate constant of process (C) is sensitive to substrate (MgATP) concentrations. By correlating our results with the cross-bridge cycle deduced from studies on extracted and reconstituted muscle proteins (e.g., Lymn and Taylor, 1971), we were able to show that process (C) involves the binding of MgATP to rigorlike cross-bridges and the actomyosin dissociation which follows the binding (Kawai, 1978, 1979, 1982). From these studies we deduced the second order rate constant of the MgATP binding and the first order rate constant of actomyosin dissociation. Goldman et al. (1982, 1984) deduced the second order rate constant by using photo labile "caged ATP" to introduce a sudden increase in the MgATP concentration within a fiber in which rigor is induced. These results on skinned fibers and results obtained from solution studies generally showed the rate constants to agree within an order of magnitude, indicating that the steps involved in substrate binding and actomyosin dissociation may not be seriously influenced by the length change (reviewed by Goldman, 1987). Physiological studies primarily used rabbit psoas fibers, but in our experience very similar kinetics were seen in

0006-3495/89/04/595/09 $2.00

fast twitch skeletal muscles (Kawai and Brandt, 1980; Kawai and Schachat, 1984; Feit et al., 1985).

If one defines the MgATP binding as the beginning of the energy transduction, the desorption of MgADP marks the end of the transduction. Although the desorption reaction is likely to be reversible, this point is not firmly established in skinned fiber systems. Sleep and Hutton (1980) demonstrated that the intermediate hydrolysis product with ADP bound to acto-S1 (S1 = myosin subfragment one) is an energetically different state from acto-S1 which has bound exogenously added MgADP. There is no doubt, however, that exogenously added ADP occupies the same location as the substrate site on myosin head, and, therefore, the ADP may behave as a competitive inhibitor in both extracted protein systems (Highsmith, 1976; Greene and Eisenberg, 1980*a*) and in skinned fiber systems (Cooke and Pate, 1985; Kawai, 1986; Schoenberg and Eisenberg, 1987). Because MgADP appears to have a comparable association constant to MgATP with the myosin head, the study of competitive inhibition can be readily achieved with this compound in the presence of equimolar concentrations of MgATP.

As a step to create a cross-bridge scheme that is consistent with our sinusoidal analysis technique, we study the effect of MgATP and MgADP on fast process (C), and examine the results in terms of elementary steps involved in the cross-bridge cycle. A preliminary account of the present result was reported (Kawai and Cornacchia, 1988).

MATERIALS AND METHODS

Chemicals and solutions

H_4EGTA [ethylene glycol-*bis* (β-amino-ethyl ether) *N,N'*-tetraacetic acid], Na_2H_2ATP (adenosine 5'-triphosphate), $Na_{1.5}H_{1.5}ADP$ (adenosine 5'-diphosphate), Na_2CP (creatine phosphate), CK (creatine kinase), A_2P_5 [p^1,p^5-di(adenosine-5') pentaphosphate], and MOPS (morpholinopropane sulphonic acid) were purchased from Sigma Chemical Co., St Louis, MO; $CaCO_3$, MgO, NaOH, KOH, KH_2PO_4, K_2HPO_4, and propionic acid from Fisher Scientific Co., Itasca, IL. All chemicals were of analytical grade or better.

The relaxing solution contained (mM): 6 EGTA, 2 MgATP, 5 free ATP, 8 Pi (inorganic phosphate), 48 K propionate, 62 Na propionate, and 10 MOPS. The wash solution contained 0.3 MgATP, 8 Pi, 103 K propionate, 75 Na propionate, and 10 MOPS. Control activating solution contained 6 CaEGTA, 5.1 MgATP, 5.17 free ATP, 15 CP, 8 Pi, 29 K propionate, 26 Na propionate, 10 MOPS, and 80 U/ml CK. The solution composition of each individual experiment is found in the Results section. When the effect of a specific compound was studied, its concentration was increased in one group of experiments, and decreased in the other group, so that the averaged results contained about half of each group. In this way, one can minimize systematic errors due to progressive deterioration of the fibers (if any). In all solutions used for experiments, total Na concentration was maintained at 76 mM, the ionic strength was adjusted to 195 mM with Na/K propionates, and pH was adjusted to 7.00 ± 0.01. EGTA, CaEGTA, Pi were added as neutral K salts; MgATP, CP as neutral Na salts; ADP as $Na_{1.5}K_{1.2}ADP$; and free ATP was added as $Na_2K_{1.7}ATP$.

Individual concentrations of multivalent ionic species were calculated using our computer program, which assumed multiple equilibria with the following apparent association constants (log values at pH 7.00): CaEGTA, 6.28; MgEGTA, 1.61; CaATP, 3.70; MgATP, 4.00; CaADP, 2.65; MgADP, 2.84; CaCP, 1.15; MgCP, 1.30. pCa of activating solutions was in the range 4.5–5.0, and the experiments were performed at 20.0 ± 0.2°C.

Fiber preparations

Fiber bundles (~30 mm in length and 1 mm in diameter) were tied to bamboo sticks at body length with silk threads and were removed from the psoas muscle of 3–6–kg New Zealand White rabbits. The bundles were chemically skinned in a solution containing (mM): 5 EGTA, 2 MgATP, 5 free ATP, 132 K propionate, and 6 imidazole (ph 7.0) at 0–2°C. After 48 h in skinning solution, the bundles were transferred to a storage solution containing (mM): 5 EGTA, 2 MgATP, 5 free ATP, 132 K propionate, 6 imidazole (pH 7.0), and 6 M glycerol (50%), and kept at −20°C without freezing. Single fibers about 20 mm in length were dissected from the stock bundles and used for the experiments.

One end of the fiber was connected to a length driver, and the other end to a tension transducer by wrapping the ends of the fiber to specially designed clamps made of stainless-steel wires (0.36 mm diameter) as described. The sarcomere length was adjusted to 2.5 μm by optical diffraction using a He-Ne laser (Spectra Physics, Mountain View, CA). At this point the fiber length (L_0) was measured. The cross-sectional area of the individual fiber was estimated by measuring two diameters with an ocular micrometer and by assuming an elliptical shape.

In a typical experiment, a single fiber was tested with the control-activating solution, then relaxed. The saline was changed with the wash solution, followed by two full volume changes of the experimental solution (500 μl each), but without CaEGTA. Complex modulus data (see below) were collected to record the baseline response, and 50 μl of 66 mM CaEGTA in 10 mM MOPS (pH 7.00) was added. The change in pH and ionic strength was minimal by this mixing. The tension started to rise quickly, and plateaued in a few seconds. The complex modulus data were then collected for the active response, and the fiber was relaxed. This procedure was repeated for a series of experimental solutions.

Transient analysis by sinusoidal length changes and extraction of kinetic parameters

The sinusoidal waveform was digitally synthesized in a minicomputer (Nova 4S, Data General Corp., Southboro, MA), which controlled the length driver via a 14-bit digital-to-analogue converter. This oscillated the length of the preparation at a small peak-to-peak amplitude (standard 0.25 %L_0) and at 17 discrete frequencies (f) ranging 0.25 to 250 Hz. Both length and tension signals were simultaneously digitized with two 15-bit analogue-to-digital converters, and the complex modulus $Y(f)$ was calculated as soon as the data became available. The complex modulus is the ratio of a stress change to a strain change represented in the frequency domain. The complex modulus data collected during relaxation were subtracted from those during activation; the primary purpose of this subtraction was to correct for extraneous pickup that is unavoidable at higher frequencies.

The frequency profile of the complex modulus data was resolved into

three exponential processes (A), (B), (C) by fitting the data to Eq. 1:

$$Y(f) = H + A/[1 + a/fi] - B/[1 + b/fi] + C/[1 + c/fi]. \quad (1)$$

We denote respective characteristic frequencies by a, b, c, and their magnitudes by A, B, C. H is a constant, and $i = \sqrt{-1}$. In this report, we focus on process (C): $2\pi c$ is the apparent rate constant and equivalent to the rate constant of phase 2. At frequencies around c, the tension leads the length, hence the fibers absorb mechanical energy from an oscillating length driver. The details of the sinusoidal analysis technique were reported in Kawai and Brandt (1980).

RESULTS

Effect of MgADP on tension and complex modulus

Single muscle fibers were activated in a solution which contained (mM): 6 CaEGTA (pCa 4.54), 6.1 MgATP, 0–9.9 ADP, 0.3–4.1 Mg propionate, 0.2 A_2P_5, 8 Pi, 17–64 Na propionate, 7–66 K propionate, and 10 MOPS (pH 7.00). Free Mg (Mg^{2+}) concentration was maintained at 1 mM to ensure that most ATP and ADP molecules chelate Mg. CP/CK were deleted from the saline for obvious reasons. 0.2 mM A_2P_5 was added to the saline to inhibit adenyl kinase activity (Lienhard and Secemski, 1973). Only two extreme MgADP solutions (0 and 8 mM) were prepared initially, and solutions with intermediate concentrations were created by mixing these two. Our computer calculation of this mixing showed that the error due to rearrangement of ionic species is negligible for all practical purposes.

Fig. 1 represents isometric tension plotted against MgADP concentration. Tension was normalized against that from control activation, and the data were averaged over eight experiments. As seen in this figure, the tension was not a strong function of MgADP concentration, and it slightly increased (but insignificantly) with an increase in MgADP concentration. Our result at 20°C contrasts to that of Cooke and Pate's experiment (1985) on glycerinated rabbit psoas, in which they observed ~25% increase in isometric tension as 4–8 mM MgADP was added to the activating saline at 10°C.

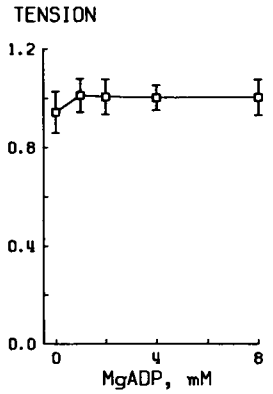

FIGURE 1 The effects of MgADP on isometric tension. Data are normalized to the tension of the control activation before averaging. The tension of the control activation was, on the average, 0.18 ± 0.01 MN/m² (n = 7, SEM). Error bars correspond to SEM over seven experiments.

Fig. 2 plots complex modulus in Nyquist plots in panel *A*, and phase shift vs. frequency in panel *B*. The numbers in the figure indicate the millimolar concentration of MgADP. As seen in the Nyquist plot, an addition of MgADP to the activating solution noticeably diminished the magnitude of processes (A) and (B) (Fig. 2 *A*) as represented by a decrease in the diameter of the corresponding arc. In Fig. 2 *B*, it is seen that the addition of MgADP shifts the phase-frequency plot gradually to the left along the frequency axis, indicating that the rate constants of processes (B) and (C) diminish with MgADP.

The complex modulus data are fitted to Eq. 1 to extract the rate constant, and the results are shown in Fig. 3. As expected, the rate constant $2\pi c$ gradually declined with an increase in the MgADP concentration.

We observed, without exception, that the longevity of fibers became poorer in solutions which contained ADP, and this effect was enhanced in solutions which contained excess Mg^{2+}.

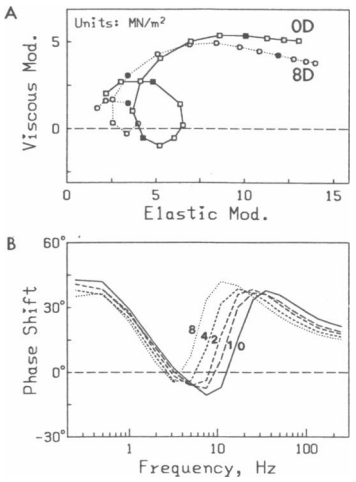

FIGURE 2 The effect of MgADP is examined in Nyquist plots in *A*, and in phase shift vs. frequency plots in *B*. The mM concentration of MgADP is as indicated in the figure. Experiments were carried out with discrete frequency points (0.25, 0.5, *1*, 2, 3.1, 5, 7.5, *11*, 17, 25, 35, 50, 70, *100*, 135, 186, 250 Hz; italicized frequencies correspond to filled symbols in *A*), and straight lines are drawn to connect them. Each curve is based on the average of eight experiments.

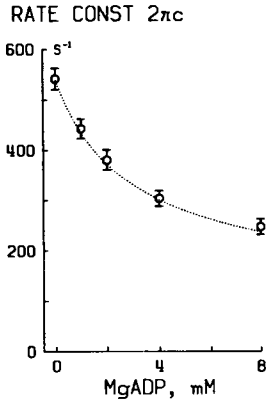

FIGURE 3 The effect of MgADP on the rate constant $2\pi c$, shown in s^{-1}. Data are averaged over eight experiments and plotted with SEM error bars. The continuous line represents the theoretical curve based on the Eq. 3 and constants in the second column of Table 1.

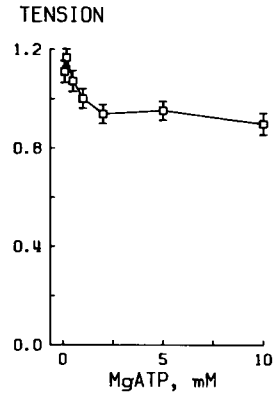

FIGURE 4 The effects of MgATP on isometric tension. The data are normalized to the tension of the control activation before averaging. The tension of the control activation was, on the average, 0.19 ± 0.02 MN/m^2 (n = 13, SEM). Error bars correspond to SEM over 6–13 experiments. The number of observations for each MgATP concentration is as follows: 0.1 mM (13), 0.2 (8), 0.5 (13), 1 (13), 2 (11), 5 (12), and 10 mM (13).

Effect of MgATP

The effect of MgATP (substrate) was studied in the presence of (mM): 6 CaEGTA (pCa 4.97), 0–10.2 MgATP, 5.1–5.3 excess (free) ATP, 8 Pi, 15 CP, 24–35 K propionate, 16–36 Na propionate, 10 MOPS (pH 7.00), 80 U/ml CK. As in the ADP studies, two extreme MgATP solutions (0 and 10 mM) were prepared, and solutions with intermediate concentrations were created by proper mixing of the two extreme solutions without significantly affecting the other ionic constituents.

The isometric tension declined with an increase in the MgATP concentration (Fig. 4). This is a significant decline, and consistent with earlier reports on both crayfish walking leg muscles and rabbit psoas. In the Nyquist plots (Fig. 5 *A*), it is seen that the magnitude of process (B) significantly increases with an increase in the substrate concentration. This is accompanied by the right shift of the phase-frequency plots in the middle and high frequency ranges (Fig. 5 *B*). When the rate constant $2\pi c$ is plotted against MgATP concentration (Fig. 6), it is seen that this rate constant increases linearly in the range 0.1–2 mM, and it saturates in the higher range (5–10 mM). The results are consistent with our earlier reports, which used Na_2SO_4 to maintain the ionic strength. Thus, it can be concluded that the effects of MgATP and MgADP are opposite in all respects.

The longevity of fibers was excellent in solutions which contained CP and CK, and it was even improved in the presence of 5 mM excess ATP.

Cross-bridge scheme

Under the conditions of these experiments, the complete cross-bridge cycle operates at a steady-state rate defined by the slowest step in the overall scheme. The minute perturbations of the sinusoidal oscillation (0.25% peak-to-peak) then permit the faster reactions to be studied as uncoupled pieces of the total scheme (Hammes, 1968). Process (C), the fastest observable process, is then coupled only to nearby steps that are even faster. The qualitative behavior of $2\pi c$ with variations of MgATP

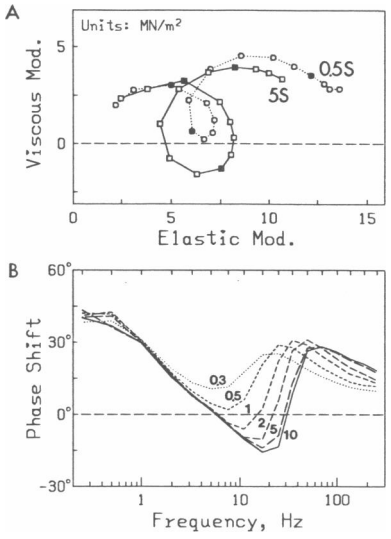

FIGURE 5 The effect of MgATP is examined in Nyquist plots in *A*, and in phase shift vs. frequency plots in *B*. The millimolar concentration of the substrate is as indicated in the figure. Frequency points used for the measurements are indicated across the top of *B*. Other details are the same as those in Fig. 2. Each curve is based on the average of eight experiments.

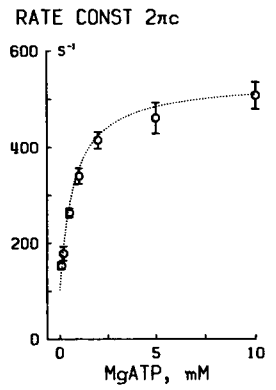

FIGURE 6 The effect of MgATP on the rate constant $2\pi c$, shown in s^{-1}. Data are averaged over 6–13 experiments and plotted with SEM error bars. The number of observations for each MgATP concentration is the same as that in Fig. 4. The continuous line represents the theoretical curve based on Eq. 3 and constants in the first column of Table 1.

concentration (S) and MgADP concentration (D) is then summarized in the following scheme:

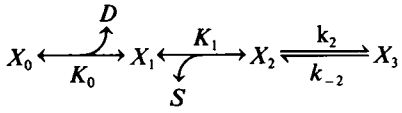

Scheme 1

In this scheme the X_j ($j = 0, 1, 2, 3$) denote cross-bridge states. The rate constants k_2 and k_{-2} describe the $X_2 - X_3$ interconversion, which we assume is the step with length sensitivity and is observed in process (C). K_1 is the equilibrium association constant for binding S to X_1. K_0 is the analogous constant for binding D to X_1. These binding steps are assumed to be sufficiently rapid with respect to step 2 that they can be taken to be at equilibrium. (The equilibrium is with respect to these states only. The overall distribution, including additional cross-bridge states, is defined by the steady-state condition. The application of the Hammes' treatment requires only that the population of these states be stationary.)

Scheme 1 has one apparent rate constant for the tension response to a small length perturbation, whether the perturbation is a step function (resulting in an exponential advance of tension over length) or a sinusoidal function (phase advance). The master equation which describes the kinetics of Scheme 1 is

$$\dot{X}_0 + \dot{X}_1 + \dot{X}_2 = -k_2X_2 + k_{-2}X_3. \quad (2)$$

Because $X_0 = K_0DX_1$, $X_2 = K_1SX_1$, and $X_0 + X_1 + X_2 + X_3 = X_T(S, D)$ = constant of time for the fast length changes used to measure process (C), the expression for the apparent rate constant can be developed from Eq. 2:

$$2\pi c = k_2K_1S/(1 + K_0D + K_1S) + k_{-2}, \quad (3)$$

under the supposition that S and D are greater than X_j ($j = 0, 1, 2$; "ligand buffering"). In the absence of D (e.g., experiments which changed MgATP concentrations), step 0 makes no contribution to the observed effect. Eq. 3 can be also derived with the relaxation kinetics approach directly as outlined by Hammes (1968). Despite the similarity of Eq. 3 to a Michaelis-Menten expression, K_0 and K_1 are association constants (unlike K_M), and site concentration (X_T) does not appear.

Values for the constants in Eq. 3 were obtained by fitting the expression to the experimental values of $2\pi c$ by least squares. The results are summarized in Table 1. The continuous lines in Figs. 3 and 6 represent Eq. 3 with these parameters. As seen in the figures, the agreement is generally satisfactory.

The association constant K_1 was first determined for individual experiments which changed MgATP concentrations by assuming K_0D was negligible compared to K_1S, and then all K_1 were averaged. The averaged K_1 ($=1.4$ mM^{-1}) was in turn used to determine K_0 for individual experiments which changed MgADP concentrations, and then K_0 was averaged. Table 1 lists all the constants which were determined similarly. It is seen in this table that k_2 determined from experiments which changed MgATP and MgADP concentrations coincide rather well, in spite of two vastly different solution conditions. The same is true for k_{-2}. These facts demonstrate a high degree of reliability of the use of Scheme 1 and Eq. 3 to account for the rate constant of process (C).

TABLE 1 Summary of association constants and rate constants

Constant	MgATP experiment	MgADP experiment	Units
	Mean ± SEM	*Mean ± SEM*	
N	13	7	
K_0		2.8 ± 0.4	mM^{-1}
K_1	1.4 ± 0.2	*	mM^{-1}
k_2	440 ± 30	470 ± 40	s^{-1}
K_1k_2	570 ± 80		mM^{-1} s^{-1}
k_{-2}	100 ± 10	130 ± 20	s^{-1}
$K_2 = k_2/k_{-2}$	4.9 ± 0.8	4.3 ± 0.8	

See Scheme 1 for definition of the constants.
*$K_1 = 1.4$ mM^{-1} is assumed.

DISCUSSION

Role of nucleotides in the cross-bridge kinetics and identity of X_0, X_1, X_2

The most important observation in the present report is that the effects of MgATP and MgADP on the rate

constant $2\pi c$ are opposite, and the rate constant results fit well to the kinetic scheme 1 (Figs. 3 and 6). From this observation, we infer that exogenously added MgADP serves as a competitive inhibitor of MgATP. This conclusion is consistent with that of Cooke and Pate (1985), Kawai (1986), and Schoenberg and Eisenberg (1987). Henceforth, there is no difficulty in identifying the state X_1 as the AM state, where A = actin and M = myosin, because it is the state without bound nucleotides. We can then identify the state X_0 as AMD, and the state X_2, as AMS. The AM state may not be equivalent to the "rigor" state that is induced by removal of MgATP, hence it is called "rigorlike" state.

Nucleotide binding steps

The association constant K_1 of MgATP to rigorlike cross-bridge X_1 is 1.4 mM^{-1} (Table 1), and agreement is seen with biochemical studies using acto-S1 (1–2 mM^{-1}; Marston and Taylor, 1980; Taylor, 1986; Millar and Geeves, 1988). The composite rate constant K_1k_2 reflects both the substrate binding and the subsequent reaction. Its value (0.57×10^6 $M^{-1}s^{-1}$) is lower than previous estimates ($1–3 \times 10^6$ $M^{-1}s^{-1}$; Kawai, 1979, 1982), because the previous estimates employed the Michaelis-Menten equation, which ignored the back reaction, $X_3 \rightarrow X_2$. Inclusion of the back reaction lowers the composite rate constant by two to three times, because it is equivalent to the initial slope of the rate constant vs. substrate relationship. The larger previous estimates may also relate to the fact that sulfate was used as the major anion instead of propionate. Our new estimate is in closer agreement with the results ($0.19–0.5 \times 10^6$ $M^{-1}s^{-1}$) of Goldman et al. (1982, 1984) who employed photolysis of caged ATP to induce a tension transient in rabbit psoas fibers. Rate constants in skinned fibers are slightly lower than those observed in solution studies of isolated proteins ($1–4 \times 10^6$ $M^{-1}s^{-1}$) (White and Taylor, 1976; Johnson and Taylor, 1978; Millar and Geeves, 1983).

The association constant K_0 of MgADP to X_1 is 2.8 mM^{-1} (Table 1), corresponding to a dissociation constant of 360 μM. This compares with 200–300 μM based on force-velocity experiments during isotonic contraction at 10°C (Cook and Pate, 1985), with 250 μM based on caged ATP experiments during isometric contraction (Danzig et al., 1986), and with 60 μM based on rapid stretch experiments (Schoenberg and Eisenberg, 1987); all these experiments used skinned or glycerinated fibers from rabbit psoas. It is rather surprising to find that the dissociation constants are in such close agreement, considering the diverse methods used for these measurements. The dissociation constant of MgADP is in the general range (60–200 μM) on extracted acto-S1 (Highsmith, 1976; Greene and Eisenberg, 1980*a*) or on myofibrils (Johnson and Adams, 1984).

Cross-bridge dissociation and identity of X_3

A few complications arise in attempting to relate this work to biochemical studies. For the work reported here and other studies of skinned fibers, it is legitimate to treat the actomyosin dissociation as a formal conformational change or isomerization, because the intracellular protein concentrations are fixed. Solution studies of muscle proteins necessarily treat actomyosin dissociation as an intermolecular process, requiring some estimate of concentrations to relate the two kinds of studies. Because of this, the idea of "effective" actin concentration (Brenner et al., 1986; Pate and Cooke, 1988) is developed to be used with the skinned fiber systems and to bridge the data with those obtained from solution studies.

A second complication is the problem of the ionic strength (IS) difference. Whereas solution studies are carried out in low IS (~40 mM), skinned fiber work is carried out in physiological IS (~195 mM). Thus, a proper adjustment is needed to compensate for this difference. Greene et al. (1983) observed IS dependence of actin-S1 association in the range 12 and 60 mM in rabbit skeletal muscles at 25°C and in the presence of ATP. They reported that the log of the association constant is linearly related to $\sqrt{IS}$ (their Fig. 5), satisfying the Dubye-Hückel limiting law. If we extrapolate their data further to IS = 195 mM, then an association constant of ~10 M^{-1} will result. If the effective actin concentration of 5 mM (Pate and Cooke, 1988) is used, then the actomyosin dissociation constant in the presence of MgATP is calculated to be ~20. This agrees approximately with the dissociation constant of "weakly attached" cross-bridges, which is estimated to be in the order of 10 from the results of Schoenberg (1988).

A third complication is that the step 2 ($X_2 \leftrightarrow X_3$) may be a composite reaction. According to Marston and Taylor (1980), acto-S1 isomerizes after the MgATP binding and before the actomyosin dissociation, as evidenced by fluorescence enhancement (see also Trybus and Taylor, 1982; Geeves et al., 1986; Taylor, 1986; Millar and Geeves, 1988). The forward rate constant for the isomerization is 1,000–5,000 s^{-1} in solution studies, with an equilibrium constant of ~10^4. The dissociation rate may be comparable or even faster. Schoenberg (1988) gives ~3,000 s^{-1} for cross-bridge detachment from the weakly attached state in skinned fibers (5°C, IS = 160 mM, no Ca). Because our value for k_2 is 440 s^{-1} (Table 1), it becomes important to relate the observations. We assume that the isomerization likewise takes

place in skinned fibers. We begin by rewriting the first-order step of Scheme 1 as two sequential steps:

$$\cdots X_2 \underset{k_{-2a}}{\overset{k_{2a}}{\rightleftharpoons}} X_{2a} \underset{k_{-2b}}{\overset{k_{2b}}{\rightleftharpoons}} X_3,$$

Scheme 2

permitting the explicit identification of X_{2a} as the species existing after the isomerization and X_3 as the detached state. It is important to note that Scheme 2 is introduced in an effort to correlate our skinned fiber results to those of biochemical studies, and the experiments reported here provide no direct evidence on the existence of X_{2a}.

In Scheme 2, if step 2a is much faster than 2b, then $k_2 = k_{2b}$, $k_{-2} = k_{-2b}$, and K_1 in Table 1 refers to $K_1/(1 + 1/K_{2a})$. In this case, our conclusion would be that the actomyosin dissociation (in the presence of MgATP) is sensed by process (C), and that this reaction is an order of magnitude slower in skinned fibers. The rate constant of reverse dissociation (k_{-2b}) is 100–130 s^{-1}, and it compares with ~200 s^{-1}, an estimate based on the equilibrium constant (~20) and the rate constant (~4,000 s^{-1}) of dissociation from solution studies. Thus, the rate constants of reattachment are similar in skinned fibers and in solution studies. The equilibrium constant K_2 (4.3–4.9, Table 1) is one quarter to half of the estimated value (10–20) based on solution studies. If we use the effective actin concentration of 5 mM, then the association constant for actomyosin becomes ~40 M^{-1} with our measurements.

If step 2b is much faster than step 2a, then $k_2 = k_{2a}$ and $k_{-2} = k_{-2a}/(1 + K_{2b})$ will result. In this case, the isomerization of the nucleotide-bound actomyosin is sensed by process (C), and this reaction is an order of magnitude slower in skinned fibers. If $K_{2b} = 20$ is used, then for the isomerization step, $k_{2a} = 440$ s^{-1}, $k_{-2a} = 2{,}100$ s^{-1}, and $K_{2a} = 0.21$ will result.

The third possibility is that there may be a condition in which both steps 2a and 2b are fast, yet the observed rate constant is slow. This actually happens when the equilibrium 2a is moderately to the left ($k_{2a} < k_{-2a}$), and the equilibrium 2b is strongly to the right ($k_{2b} \gg k_{-2b}$), so that the intermediate X_{2a} is in vanishingly small concentration (Castellan, 1963). It is also necessary that $k_{2b} > k_{2a}$. Under these conditions, $k_2 = r \cdot K_{2a}$ and $k_{-2} = r/K_{2b}$ will result, where $r = k_{-2a}k_{2b}/(k_{-2a} + k_{2b})$. The following set of numbers simulate these conditions: $k_{2a} = 1{,}000$ s^{-1}, $k_{-2a} = 5{,}000$ s^{-1}, $k_{2b} = 4{,}000$ s^{-1}, and $k_{-2b} = 200$ s^{-1}. From these, we calculate $r = 2{,}222$ s^{-1}, $K_{2a} = 0.2$, $K_{2b} = 20$, $k_2 = 444$ s^{-1}, and $k_{-2} = 111$ s^{-1}. In this simulation the results agree with our observations. All rate constants have reasonable correlations with those from biochemical studies, except for k_{-2a}. A large number is assigned to k_{-2a}, which results in a low K_{2a}.

In all cases discussed above, we cannot use the equilibrium constant for the isomerization step (K_{2a}) known from solution studies (~10^4, Taylor, 1986) to account for skinned fiber results. Combined with K_{2b} = 10–20, this will shift the equilibrium in Scheme 2 highly towards the right, i.e., dissociation, when millimolar concentrations of MgATP are present. We know that this does not happen in skinned fibers, because ~57% of cross-bridges are attached during maximal activation based on our stiffness measurement (Kawai, 1982). Thus, it is not unexpected if K_{2a} is found to be in the order of one in skinned fibers. We can visualize this, because in skinned fibers the head is confined in an ordered array of filaments and its mobility is limited, causing an alteration in the kinetics of the isomerization step.

The preceding argument shows that some modifications of the constants obtained from biochemical studies are essential to account for the data obtained from skinned fiber studies. Among three cases discussed above, the first two cases require reduction in the rate constants by ~10-fold. The last case requires the least amount of modification, although the mechanism is complex. Since any one of these are possible, we identify step 2 ($X_2 \leftrightarrow X_3$) in Scheme 1 as the isomerization/dissociation step, and X_3 as the detached state.

Insensitivity of process (C) to phosphate concentration

Some constraints derive from the insensitivity of $2\pi c$ to reported changes in phosphate (Pi) concentration (Kawai, 1986; Kawai et al., 1987). This simple experimental observation means that intervening slow steps isolate each end of Scheme 1 or 2 from Pi dissociation. At millimolar concentrations, the elementary Pi binding process can be assumed to be rapid, with limitations arising from conformational changes. Thus, we can conclude that the cross-bridge state X_3 is isolated from the Pi step by a slower reaction(s), hence X_3 comes earlier than the Pi-release step along the hydrolysis route. This is consistent with the assumption of Scheme 2. X_3 most likely includes all the detached states which are identified as intermediate hydrolysis products; it may also include "weakly attached" states (Greene and Eisenberg, 1980*b*), because these are likely to be registered as detached cross-bridges.

Closing of the cross-bridge cycle

The cross-bridge Scheme 1 or 2 as presented takes the form of chain reactions, whereas the complete cross-

bridge reaction is a cycle. Then a question arises: what happens if a reaction $X_3 \rightarrow X_0$ (or $X_3 \rightarrow X_1$) is added to the scheme to close the cross-bridge cycle? A mathematical evaluation of such a cyclical scheme proves that the argument above remains quantitatively the same so long as the closing reaction includes a much slower step(s) than $2\pi c$. Based on this consideration and on the fit of our results to Eq. 3 (Figs. 3 and 6), we conclude that very slow steps such as the rate-limiting step are excluded from the elementary steps outlined within Scheme 1 or 2. This is consistent with the observation that the rate constant $2\pi c$ is $>100\ s^{-1}$ (Fig. 6), and is much faster than the rate-limiting step which is in the order of $1\ s^{-1}$ (Curtin et al., 1974; Levy et al., 1976; Arata et al., 1977; Takashi and Putnam, 1979; Glyn and Sleep, 1985; Kawai et al., 1987) as determined from the ATP turnover number. Note that the increase in the turnover number with the length oscillation is limited to ~6% in rabbit psoas at 100 Hz and at ~1% L_0 (Kawai et al., 1987), hence the presence of oscillation at an amplitude of 0.25% L_0 should not modify this conclusion.

We initiated this study to develop an independent cross-bridge scheme in a skinned fiber system, which would be consistent with the results of sinusoidal analysis experiments. Our results indicate that the scheme thus developed parallels those known from biochemical studies. Some constants are shown to be common to both systems, while others are shown to be different. These studies will undoubtedly aid in determining the elementary step(s) influenced by strain, i.e., the coupling between the chemical events and the mechanical events in muscular contraction.

The authors are grateful to Mr. Thomas W. Cornacchia and Mr. Richard W. Arbuckle for their excellent technical assistance.

The present work was supported by grants from the National Institutes of Health (AR21530 to M. Kawai; GM23302 to H. R. Halvorson) and the National Science Foundation (DCB87-96283 to M. Kawai). M. Kawai is an established investigator of the American Heart Association.

Received for publication 19 May 1988 and in final form 26 September 1988.

REFERENCES

Arata, T., Y. Mukohata, and Y. Tonomura. 1977. Structure and function of the two heads of the myosin molecule. VI. ATP hydrolysis, shortening, and tension development of myofibrils. *J. Biochem. (Tokyo).* 82:801–812.

Brenner, B., L. C. Yu, L. E. Greene, E. Eisenberg, and M. Schoenberg. 1986. Ca^{2+}-Sensitive cross-bridge dissociation in the presence of magnesium pyrophosphate in skinned rabbit psoas fibers. *Biophys. J.* 50:1101–1108.

Castellan, G. W. 1963. Calculation of the spectrum of chemical relaxation times for a general reaction mechanism. *Ber. Bunsen-Ges Phys. Chem.* 67:898–908.

Cooke, R., and E. Pate. 1985. The effect of ADP and phosphate on the contraction of muscle fibers. *Biophys. J.* 48:789–798.

Cooke, R., M. S. Crowder, and D. D. Thomas. 1982. Orientation of spin-labels attached to cross-bridges in contracting muscle fibers. *Nature (Lond.).* 300:776–778.

Curtin, N. A., C. Gilbert, K. M. Kretzschmar, and D. R. Wilkie. 1974. The effect of the performance of work on total energy output and metabolism during muscular contraction. *J. Physiol. (Lond.).* 238:455–472.

Danzig, J. A., D. R. Trentham, and Y. E. Goldman. 1986. Kinetics of activation of skeletal muscle fibers by photolysis of caged ATP in the presence of MgADP. *Biophys. J.* 49:268a. (Abstr.)

Feit, H., M. Kawai, and M. I. Schulman. 1985. Stiffness and contractile properties of avian normal and dystrophic muscle bundles as measured by sinusoidal length perturbations. *Muscle & Nerve.* 8:503–510.

Geeves, M. A., T. E. Jeffries, and N. C. Millar. 1986. ATP-induced dissociation of rabbit skeletal actomyosin subfragment 1. Characterization of an isomerization of the ternary acto-S1-ATP complex. *Biochemistry.* 25:8454–8458.

Glyn, H., and J. Sleep. 1985. Dependence of adenosine triphosphatase activity of rabbit psoas muscle fibres and myofibrils on substrate concentration. *J. Physiol. (Lond.).* 365:259–276.

Goldman, Y. 1987. Kinetics of the actomyosin ATPase in muscle fibers. *Annu. Rev. Physiol.* 49:637–654.

Goldman, Y. E., M. G. Hibberd, J. A. McCray, and D. R. Trentham. 1982. Relaxation of muscle fibres by photolysis of caged ATP. *Nature (Lond.).* 300:701–705.

Goldman, Y. E., M. G. Hibberd, and D. R. Trentham. 1984. Initiation of active contraction by photogeneration of adenosine-5'-triphosphate in rabbit psoas muscle fibres. *J. Physiol. (Lond.).* 354:605–624.

Greene, L. E., and E. Eisenberg. 1980*a*. Dissociation of the actin · subfragment 1 complex by adenyl-5'-*yl* imidodiphosphate, ADP, and PP_i. *J. Biochem.* 255:543–548.

Greene, L. E., and E. Eisenberg. 1980*b*. Cooperative binding of myosin subfragment-1 to the actin-troponin-tropomyosin complex. *Proc. Natl. Acad. Sci. USA.* 77:2616–2620.

Greene, L. E., J. R. Sellers, E. Eisenberg, and R. S. Adelstein. 1983. Binding of gizzard smooth muscle myosin subfragment 1 to actin in the presence and absence of adenosine 5'-triphosphate. *Biochemistry.* 22:530–535.

Hammes, G. G. 1968. Relaxation spectrometry of biological systems. *Adv. Protein Chem.* 23:1–57.

Heinl, P., H. J. Kuhn, and J. C. Rüegg. 1974. Tension responses to quick length changes of glycerinated skeletal muscle fibres from the frog and tortoise. *J. Physiol. (Lond.).* 237:243–258.

Highsmith, S. 1976. Interactions of actin and nucleotide binding sites on myosin subfragment one. *J. Biol. Chem.* 251:6170–6172.

Huxley, A. F., and R. M. Simmons. 1971. Proposed mechanism of force generation in striated muscle. *Nature (Lond.).* 233:533–538.

Johnson, K. A., and E. W. Taylor. 1978. Intermediate states of subfragment 1 and actosubfragment 1 ATPase: reevaluation of the mechanism. *Biochemistry.* 17:3432–3442.

Johnson, R. E., and P. H. Adams. 1984. ADP binds similarly to rigor muscle myofibrils and to actomyosin-subfragment one. *FEBS (Fed. Eur. Biochem. Soc.) Lett.* 174:11–14.

Kawai, M. 1978. Head rotation or dissociation? A study of exponential rate processes in chemically skinned rabbit muscle fibers when MgATP concentration is changed. *Biophys. J.* 22:97–103.

Kawai, M. 1979. Effect of MgATP on cross-bridge kinetics in chemically skinned rabbit psoas fibers as measured by sinusoidal analysis technique. *In* Cross-Bridge Mechanism in Muscle Contraction. H. Sugi and G. H. Pollack, editors. University of Tokyo Press, Tokyo. 149–169.

Kawai, M. 1982. Correlation between exponential processes and cross-bridge kinetics. *In* Basic Biology of Muscles: A Comparative Approach. B. M. Twarog, R. J. C. Levine, and M. M. Dewey. Raven Press, New York. 109–130.

Kawai, M. 1986. The role of orthophosphate in crossbridge kinetics in chemically skinned rabbit psoas fibres as detected with sinusoidal and step length alterations. *J. Muscle Res. Cell Motil.* 7:421–434.

Kawai, M., and P. W. Brandt. 1980. Sinusoidal analysis; a high resolution method for correlating biochemical reactions with physiological processes in activated skeletal muscles of rabbit, frog and crayfish. *J. Muscle Res. Cell Motil.* 1:279–303.

Kawai, M., and T. Cornacchia. 1988. Study of ADP-release step in chemically skinned single rabbit psoas fibers. *Biophys. J.* 53:23a. (Abstr.)

Kawai, M., and F. H. Schachat. 1984. Differences in the transient response of fast and slow skeletal muscle fibers: correlations between complex modulus and myosin light chains. *Biophys. J.* 45:1145–1151.

Kawai, M., K. Güth, K. Winnikes, C. Haist, and J. C. Rüegg. 1987. The effect of inorganic phosphate on the ATP hydrolysis rate and the tension transients in chemically skinned rabbit psoas fibers. *Pfluegers Arch. Eur. J. Physiol.* 408:1–9.

Levy, R. M., Y. Umazume, and M. J. Kushmerick. 1976. Ca^{2+} dependence of tension and ADP production in segments of chemically skinned muscle fibers. *Biochim. Biophys. Acta.* 430:352–365.

Lienhard, G. E., and I. I. Secemski. 1973. P^1,P^5-Di(adenosine-5′) pentaphosphate, a potent multisubstrate inhibitor of adenylate kinase. *J. Biol. Chem.* 248:1121–1123.

Lymn, R. W., and E. W. Taylor. 1971. The mechanism of adenosine triphosphate hydrolysis by actomyosin. *Biochemistry.* 10:4617–4624.

Marston, S. B., and E. W. Taylor. 1980. Comparison of the myosin and actomyosin ATPase mechanisms of four types of vertebrate muscles. *J. Mol. Biol.* 139:573–600.

Millar, N. C., and M. A. Geeves. 1983. The limiting rate of the ATP-mediated dissociation of actin from rabbit skeletal muscle subfragment 1. *FEBS (Fed. Eur. Biochem. Soc.) Lett.* 160:141–148.

Millar, N. C., and M. A. Geeves. 1988. Protein fluorescence changes associated with ATP and adenosine 5′-[γ-thio]triphosphate binding to skeletal muscle myosin subfragment 1 and actomyosin subfragment 1. *Biochem. J.* 249:735–743.

Pate, E., and R. Cooke. 1988. Energetics of the actomyosin bond in the filament array of muscle fibers. *Biophys. J.* 53:561–573.

Schoenberg, M. 1988. Characterization of the myosin adenosine triphosphate (M · ATP) crossbridge in rabbit and frog skeletal muscle fibers. *Biophys. J.* 54:135–148.

Schoenberg, M., and E. Eisenberg. 1987. ADP binding to myosin cross-bridges and its effect on the cross-bridge detachment rate constants. *Biophys. J.* 89:905–920.

Sleep, J. A., and R. L. Hutton. 1980. Exchange between inorganic phosphate and adenosine 5′-triphosphate in the medium by actomyosin subfragment 1. *Biochemistry.* 19:1276–1283.

Sugi, H., and T. Kobayashi. 1983. Sarcomere length and tension changes in tetanized frog muscle fibers after quick stretches and releases. *Proc. Natl. Acad. Sci. USA.* 80:6422–6425.

Takashi, R., and S. Putnam. 1979. A fluorimetric method for continuously assaying ATPase: application to small specimens of glycerol-extracted muscle fibers. *Anal. Biochem.* 92:375–382.

Taylor, E. W. 1986. Mechanism and energetics of actomyosin ATPase. *In* The Heart and Cardiovascular System. H. A. Fozzard, E. Haber, R. B. Jennings, and A. M. Katz, editors. Raven Press, New York. 789–802.

Thomas, D. D. 1987. Spectroscopic probes of muscle cross-bridge rotation. *Annu. Rev. Physiol.* 49:691–709.

Trybus, K. M., and E. W. Taylor. 1982. Transient kinetics of adenosine 5′-diphosphate and adenosine 5′-(β,γ-imidotriphosphate) binding to subfragment 1 and actosubfragment 1. *Biochemistry.* 21:1284–1294.

White, H. D., and E. W. Taylor. 1976. Energetics and mechanism of actomyosin adenosine triphosphatase. *Biochemistry.* 15:5818–5826.

Yanagida, T. 1981. Angles of nucleotides bound to cross-bridges in glycerinated muscle fiber at various concentrations of ε-ATP, ε-ADP and ε-AMPPNP detected by polarized fluorescence. *J. Mol. Biol.*146:539–560.